Thickness and Bending Effects

23

23.1. The Fundamental Ideas 369
23.2. Thickness Fringes 369
23.3. Thickness Fringes and the Diffraction Pattern 371
23.4. Bend Contours (Annoying Artifact, Useful Tool, and Invaluable Insight) 372
23.5. ZAPs and Real-Space Crystallography 373
23.6. Hillocks, Dents, or Saddles 374
23.7. Absorption Effects 374
23.8. Computer Simulation of Thickness Fringes 375
23.9. Thickness-Fringe/Bend-Contour Interactions 375
23.10. Other Effects of Bending 376

CHAPTER PREVIEW

We see diffraction contrast in an image of a perfect specimen for two reasons: either the thickness of the specimen varies or the diffraction conditions change across the specimen.

The *thickness* effect: When the thickness of the specimen is not uniform, the coupling of the direct and diffracted beams occurs over different distances, thus producing a thickness effect. Don't confuse diffraction contrast due to thickness changes with mass-thickness contrast discussed in the previous chapter. The effects are very different. The diffraction contrast changes with tilt, but the mass-thickness contrast doesn't.

The *bending* effect: Whenever the orientation of the diffracting planes changes, i.e., when the diffracting planes bend, the contrast changes. To interpret changes in image contrast we need to understand how the contrast is related to thickness and bending.

We call these two important contrast phenomena "thickness fringes" and "bend contours."

The present chapter is particularly important for three reasons:

- All TEM specimens are thin but their thickness is rarely constant.
- Because the specimens are so thin they also bend elastically, i.e., the lattice planes physically rotate.
- The planes also bend when lattice defects are introduced.

D. B. Williams et al., *Transmission Electron Microscopy*

We can see the effects of these rotations even when they are < 0.1°, since they still have a significant effect on the image contrast. Therefore, the bending may arise because the specimen is thin (i.e., giving possible artifacts of the technique) or it may be caused by strains which were present in the bulk material. The result is that, in real specimens, bending and thickness effects often occur together.

Thickness and Bending Effects

23

23.1. THE FUNDAMENTAL IDEAS

To understand the origin of thickness fringes and bend contours we limit our discussion to the two-beam situation and recall equations 13.46 and 13.47, which we derived from the Howie–Whelan equations. The intensity of the Bragg-diffracted beam is then given by

$$I_g = \left|\phi_g\right|^2 = \left(\frac{\pi t}{\xi_g}\right)^2 \left(\frac{\sin^2(\pi t s_{\text{eff}})}{(\pi t s_{\text{eff}})^2}\right) = 1 - I_0 \qquad [23.1]$$

where s_{eff} is the effective excitation error

$$s_{\text{eff}} = \sqrt{s^2 + \frac{1}{\xi_g^2}} \qquad [23.2]$$

Although we will concentrate on I_g (the DF image intensity) for most of this discussion, the direct beam (BF image) behaves in a complementary manner (neglecting, for now, the effect of absorption). The diffracted intensity is periodic in the two independent quantities, t and s_{eff}. If we imagine the situation where t remains constant but s (and hence s_{eff}) varies locally, then we produce bend contours. Similarly, if s remains constant while t varies, then thickness fringes will result.

This chapter is simply concerned with the physical understanding of equation 23.1 and how you can relate the image to the information contained in the diffraction pattern. Although these effects are often a hindrance to systematic analysis of lattice defects, they can, in certain situations, be useful. The most important reason for understanding them is that they are unavoidable!

23.2. THICKNESS FRINGES

As a result of the way that we thin TEM specimens, very few of them (only evaporated thin films or ideal ultramicrotomed sections) have a uniform thickness over their entire area. A BF/DF pair of images from the same region of a specimen at 300 kV is shown in Figure 23.1; the thin area is generally in the form of a wedge.

Consider again equation 23.1. You should remember that, in this calculation, t is not the "thickness" of the foil; it is actually the distance "traveled" by the diffracted beam. If we try to treat the many-beam situation rigorously, then the value of t would, in general, be different for each beam. If you are actually viewing the foil flat-on (i.e., one surface normal to the beam), then t will be close to the geometric thickness of the foil. However, it is more difficult to analyze the image thoroughly when the foil is wedge-shaped and inclined to the beam. We almost invariably make the approximation that t is fixed with the justification being that the Bragg angles are small.

Equation 23.1 tells us that the intensity of both the **0** and the **g** beams oscillates as t varies. Furthermore, these oscillations are complementary for the DF and BF images, as we show schematically in Figure 23.2. You can, of course, confirm this observation at the microscope by forming the image without using an objective aperture; there is then minimal contrast when you're in focus. The intensity, I_0, of the incident beam starts equal to unity and gradually decays, while the intensity of the diffracted beam, I_g, gradually increases until it becomes unity; I_0 is then zero; the process then repeats itself. In reality, the situation is complicated by the presence of other diffracted beams (we are never truly in a two-beam situation) and absorption.

> As a rule of thumb, when other diffracted beams are present the effective extinction distance is reduced. At greater thicknesses, absorption occurs and the contrast is reduced.

These oscillations in I_0 or I_g are known as thickness fringes, though they are often not fringes. We sometimes call them thickness contours, because they denote the con-

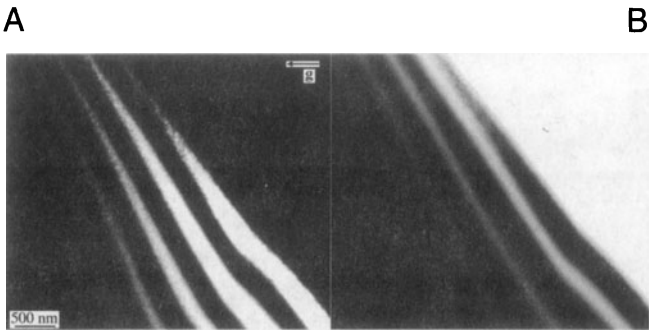

Figure 23.1. (A) DF and (B) BF images from the same region of a wedge-shaped specimen of Si at 300 kV tilted so that **g**(220) is strong. The periodicity and contrast of the fringes is similar and complementary in each image.

tours where the specimen has constant thickness; you will only see these fringes when the thickness of the specimen varies locally, otherwise the contrast will be a uniform gray. As we'll see, the actual contrast can quickly change if the specimen is tilted through a small angle.

> It is important to realize that the image may appear to be black or white depending on the thickness of the specimen.

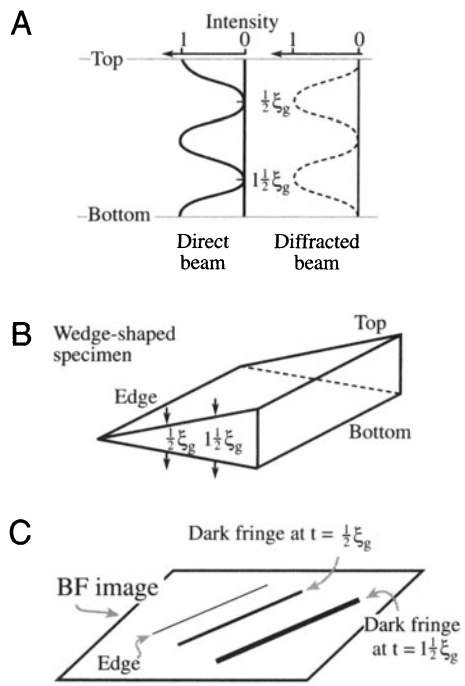

Figure 23.2. (A) At the Bragg condition (**s** = 0), the intensities of the direct and diffracted beams oscillate in a complementary way. (B) For a wedge specimen, the separation of the fringes in the image (C) is determined by the angle of the wedge and the extinction distance, ξ_g.

For example, in BF images, thicker areas are often brighter than thinner areas, which really is counterintuitive.

Several examples of how thickness fringes might appear in your image are shown in Figure 23.3. Although it is often helpful to think of these fringes as thickness con-

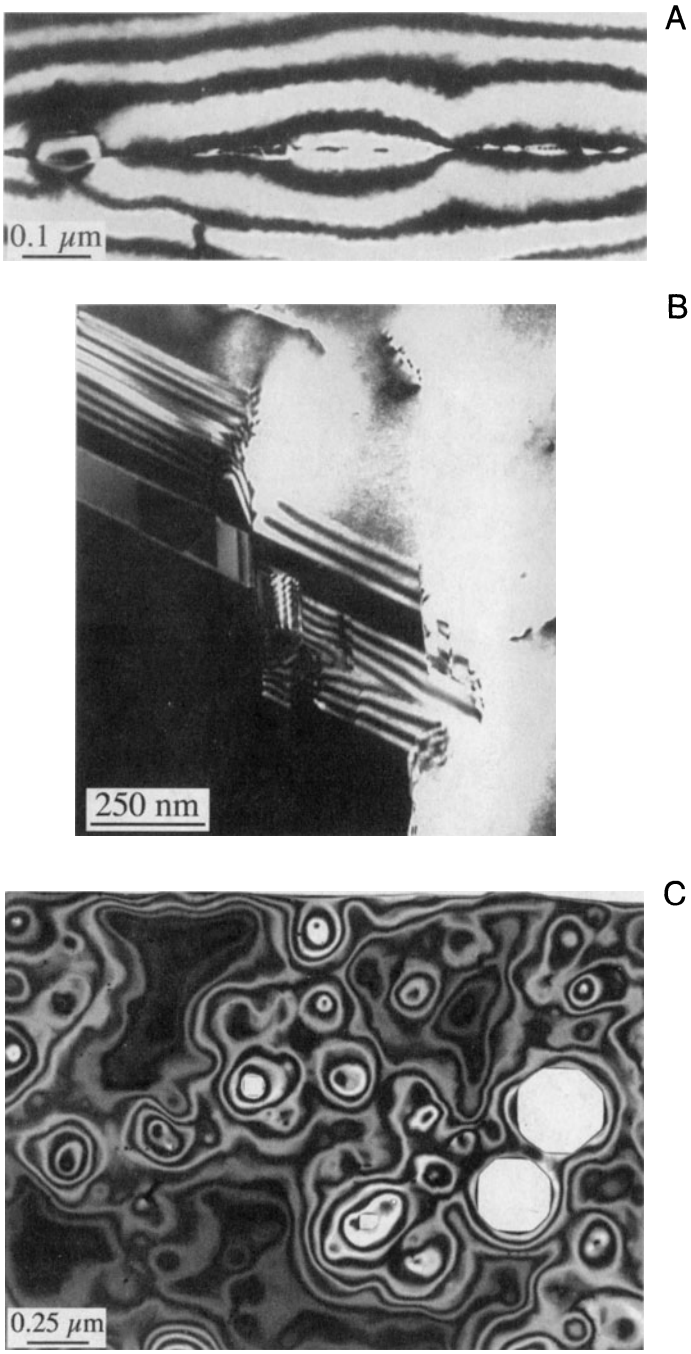

Figure 23.3. Examples of thickness fringes in (A) DF image of a preferentially thinned grain boundary; (B) a strong 220 DF image of microtwinned GaAs taken with only the left-hand grain diffracting, and (C) BF image of a chemically etched thin film of MgO. The white regions in (C) are holes in the specimen.

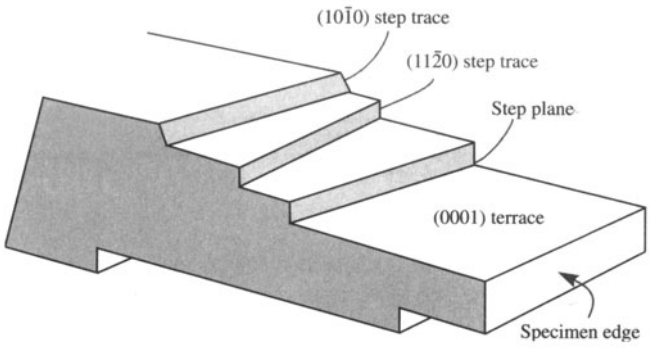

Figure 23.4. Schematic cross-sectional view of a specimen with terraces parallel to the surface and steps connecting terraces.

tours analogous to height or depth contours on a map, with the hole at sea level, remember that there are *two* surfaces to your TEM specimen. A DF image will usually appear to give greater contrast. This is partly because any hole now appears dark, but also because many-beam effects are less important in DF. In Figure 23.3A the narrow fringe pattern in this DF image is due to the grain boundary region being thinner than the matrix. In the DF image in Figure 23.3B, the reflection used to form the image is only excited in the right grain so the left grain is black; the diffracting grain exhibits strong thickness fringes in the regions where there are microtwins. This image introduces the idea that images of defects can also show thickness effects.

In Figure 23.3C, the specimen is an almost flat, parallel-sided film of MgO with holes formed by chemical etching; after thinning, the surfaces were faceted by heating the specimen at 1400°C. The holes in the image are white, so it is a BF image. The contours, like the holes, are angular because of the faceting, but they are not uniformly spaced because it's not a uniform wedge. Notice that the center of the hole is faceted and that the first fringe is a very narrow dark line. We know that this surface is different because it is curved. We also know from Figure 23.2 that, in a BF image, the first fringe must be bright if the thickness actually decreases to zero. We can therefore conclude from this one image that the specimen is not tapering to zero thickness at the center of this hole.

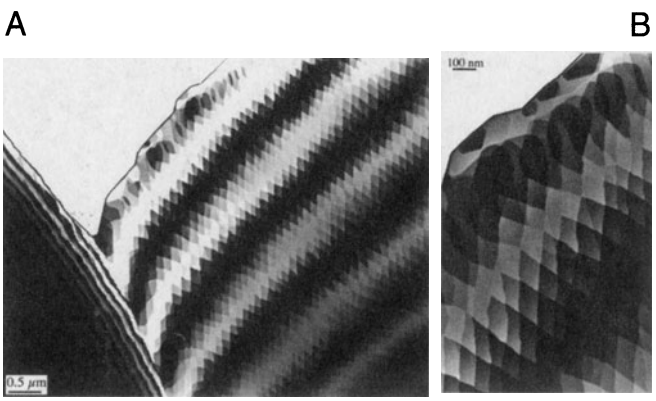

Figure 23.5. Thick fringes from an annealed Al_2O_3 specimen with the geometry shown in Figure 23.4. (A) At low magnification, the fringes are well defined and continuous, even when the wedge angle and wedge axis change. (B) At higher magnification, the contrast is seen to be quantized within a given fringe.

Although we've talked about wedges or specimens with gently curving surfaces so far, the way we actually calculate and analyze the contrast from such wedges is shown in Figure 23.4. We imagine that the specimen has two parallel surfaces which are normal to the electron beam, so that we have a fixed thickness for each calculation. We also assume that the beam is normal to the surface. We then change t and recalculate the intensity. Finally, we plot the different values for the intensity against t but we never actually inclined the surfaces!

Figure 23.5 shows a striking image of a wedge-shaped specimen of Al_2O_3 which has been heat treated so that the surface has facets parallel to certain low-index planes. The thickness fringes can then be seen to be discrete regions of different shades of gray; the fringes are, in general, quantized. You can form similar specimens by cleaving layer materials (e.g., graphite) but the specimens tend to bend, which obscures these abrupt contrast changes.

23.3. THICKNESS FRINGES AND THE DIFFRACTION PATTERN

A general rule in TEM is that, whenever we see a periodicity in real space (i.e., the image), there must be a corresponding array of spots in reciprocal space; the converse is also true. If we image a specimen with a constant wedge angle, then we will see a uniform spacing of thickness fringes in both the BF and DF two-beam images even when $\mathbf{s}_g = 0$. We must therefore have more than one spot "at G" when $\mathbf{s}_g = 0$, otherwise we would not see fringes. We already know that if we increase $\mathbf{s}$ or if the wedge angle were larger, then the fringe separation would decrease and the spacing of these spots must therefore increase.

To understand why there is more than one spot at G, go back to Chapter 17 where we showed that, because the specimen is thin, any spot in the DP will be elongated normal to the surface. When the specimen is wedge-shaped, there will be two surfaces and we can imagine the spot being elongated normal to both surfaces, as was shown in Figure 17.4. Actually, we have two curved relrods which do not intersect at $\mathbf{s} = 0$; we related this curvature to the dispersion surface in Chapter 15. The diffraction geometry close to G is shown in Figure 23.6.

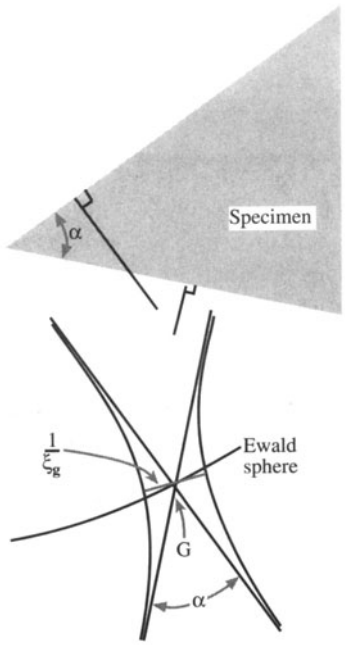

Figure. 23.6. Relrods aligned normal to both surfaces of a wedge-shaped specimen. In practice, the relrods don't cross so there are always two spots in the DP.

The minimum spot spacing in the DP corresponds to the periodicity of the thickness fringes, which at **s** = 0 is given directly by the extinction distance.

This spot spacing is thus related to ξ_g^{-1}. While the spacing of the thickness fringes depends on ξ_g, it is not equal to ξ_g. As we referenced back in Chapter 17, Amelinckx's group has shown that we can describe this geometric relationship as shown in Figure 17.4. As we tilt the crystal away from **s** = 0, the Ewald sphere will move up or down (as **s** becomes negative or positive) to cut the two "rods." So, you can see that there will be two spots instead of one at G and their separation will increase as **s** increases. As the separation increases, the spacing of the fringes decreases; the thickness fringes move closer together because the ξ_{eff} has decreased. The change in the fringe spacing is similar either side of **s** = 0.

So be wary of trying to make accurate thickness measurements in wedge-shaped crystals.

We refer to thickness fringes as being an example of amplitude contrast because, in the two-beam case, they are associated with a particular reflection, **g**. They actually occur due to interference between two beams, both of which are located close to **g**, so they are really an example of phase contrast although we rarely think of them as such.

23.4. BEND CONTOURS (ANNOYING ARTIFACT, USEFUL TOOL, AND INVALUABLE INSIGHT)

This is a particularly satisfying topic, because you can understand it by considering a simple physical picture and yet the concept involved is the basis for understanding most aspects of defect contrast. Bend contours (don't call them extinction contours) occur when a particular set of diffracting planes is not parallel everywhere; the planes rock into, and through, the Bragg condition.

The specimen shown schematically in Figure 23.7 is aligned so that the $hk\ell$ planes are exactly parallel to the incident beam at the center of the figure and always lie normal to the specimen surface even when it bends. We imagine that the foil bends evenly, so that the $hk\ell$ planes are exactly in the Bragg condition at A and the $\bar{h}\bar{k}\bar{\ell}$ planes are exactly in the Bragg condition at B. We can draw the systematic row of reflections as you see below the bent crystal. Notice that –G is now on the left and G on the right. Now if we form a BF image we will see two dark lines. Next, we form the DF image using reflection **g**. We see a

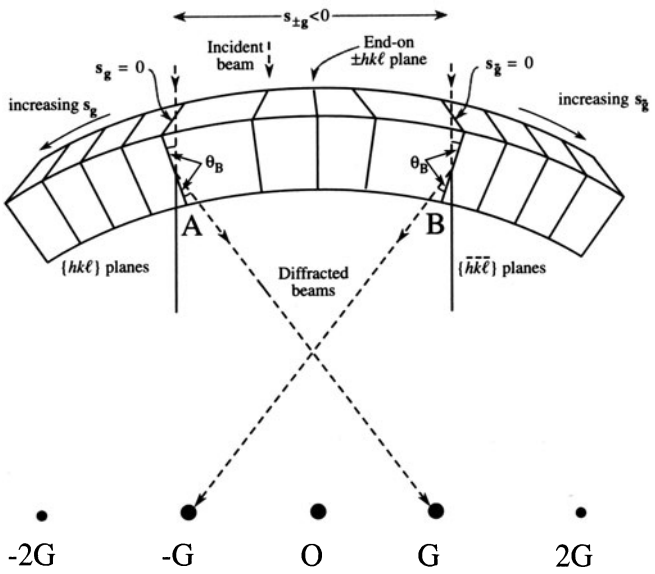

Figure. 23.7. The origin of bend contours shown for a foil symmetrically bent either side of the Bragg conditions. For this geometry, when the $hk\ell$ planes are in the Bragg condition, the reflection G is excited. Notice that G and the diffracting region are on opposite sides of O; if the foil were bent upwards, they would be on the same side.

bright band on the left because that's where **g** is excited. Now use $\bar{\mathbf{g}}$ to form the image and the bright band is on the right. These bands are referred to as bend contours. Experimental images are shown in Figures 23.8 and 23.9.

> In actually doing this imaging experiment you should translate the objective aperture to form the DF images; you'll lose some resolution but don't move the specimen.

Remembering Bragg's law, the $(2h\ 2k\ 2\ell)$ planes diffract strongly when θ has increased to $\sim 2\theta_B$. So we'll see extra contours because of the higher-order diffraction. As θ increases, the planes rotate through the Bragg condition more quickly (within a small distance Δx) so the bend contours become much narrower for higher-order reflections.

Tyro-microscopists occasionally have difficulty in distinguishing higher-order bend contours from real line defects in the crystal. The solution is very simple: tilt your specimen. Bend contours are not fixed to any particular position in the specimen and move as you tilt.

Bend contours are true amplitude contrast, not phase contrast.

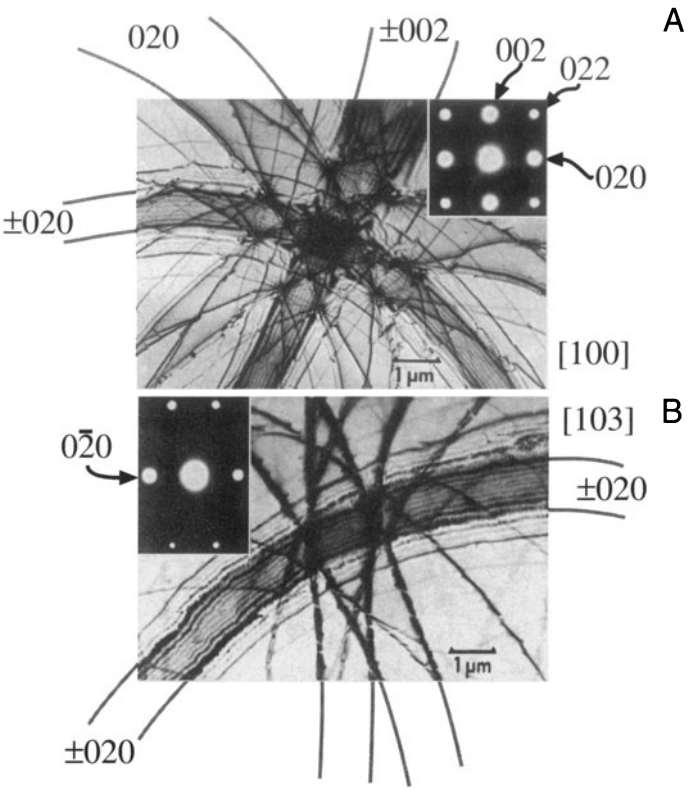

Figure. 23.8. BF images of a bent Al specimen oriented close to the (A) [100] and (B) [103] zone axes. These images are known as (real-space) ZAPs, or zone-axis patterns, and are shown with their respective zone-axis diffraction patterns (insets). Each diffracting plane produces two bend contours, depending on whether θ_B or $-\theta_B$ is satisfied. Note that the separation of the bend contours is not uniform for any particular pair of planes because the curvature of the bending is not, in general, the same.

23.5. ZAPS AND REAL-SPACE CRYSTALLOGRAPHY

In the above discussion we only considered bending about one axis. In real specimens, the bending will be more complex. This complexity will be important when the bent area is oriented close to a low-index pole, because the bend contours form a zone-axis pattern, or ZAP. Two examples of these ZAPs are shown in Figure 23.8. Although the ZAP is distorted, the symmetry of the zone axis is clear and such patterns have been used as a tool for real-space crystallographic analysis (e.g., Rackham and Eades 1977). Each contour is uniquely related to a particular set of diffracting planes, so the ZAP does not automatically introduce the twofold rotation axis that we are used to in SAD patterns. These contours are the real-space analog of the symmetry in large-angle CBED patterns.

In fact, it's the exception that a $\pm\mathbf{g}$ pair of bend contours are straight and parallel. In case you are having a problem visualizing how a pair of contours might diverge, go back to the bent specimen in Figure 23.7, hold the $\bar{h}\bar{k}\bar{\ell}$ plane fixed at $x = x_0$, and then as you move along the foil (going into the page) gradually decrease the bend in the foil. The position where the $hk\ell$ planes are in the Bragg condition gradually moves to the left, so $-x_0$ becomes more negative. Since x_0 is fixed the contours move apart in the image.

Notice how at the zone axis, the main 200 contours in the [100] ZAP are closely spaced, while in the [103] pattern, only one of contours is more closely spaced; the others are more clearly defined and further apart.

> In this case, small **g** in the DP gives a small spacing in the image, contrary to the usual inverse relationship between image and DP.

When the foil curvature is equal, this effect allows you to recognize a low-index ZAP. Since you can tilt the crystal you can form different ZAPs from exactly the same area of your specimen just as you can for SAD and CBED (where we also use the term ZAP but then it refers to a DP). You index the contours in the manner described in Section 18.4 but use all the spots in the zone-axis SAD pattern.

If your specimen is buckled, you can tilt it so that a particular bend contour stays at the position you're studying in the image. You're then doing the same operation as we did using Kikuchi lines in Chapter 19. Tilting in image mode is more tricky, but if the specimen is very buckled or too thin, you can't use Kikuchi lines. The ZAP and bend contours let you work in real space. You can even set the value of **s** for a particular **g** at a particular location on your specimen!

23.6. HILLOCKS, DENTS, OR SADDLES

The simplest use for bend contours is in determining whether an area is a hillock or a dent. This information is useful when analyzing particles grown on a substrate, particularly if the substrate is a thin film.

Figures 23.9A and B show a ZAP in a thin specimen of Al_2O_3 and the associated SAD pattern; the dark bands are $\{3\bar{3}00\}$ bend contours. Figures 23.9C–H show DF images recorded using each of these reflections; the area is identical in each of these images. Using Figures 23.7 you can determine the sense of the bending. You can see directly that the bend contour from one set of $hk\ell$ planes does not necessarily lie parallel to those planes but instead both curves and changes in width.

Remember, for these contrast experiments only, it is important that you move the objective aperture, not the specimen. The resolution of the image will be lower, but this is not critical for this application.

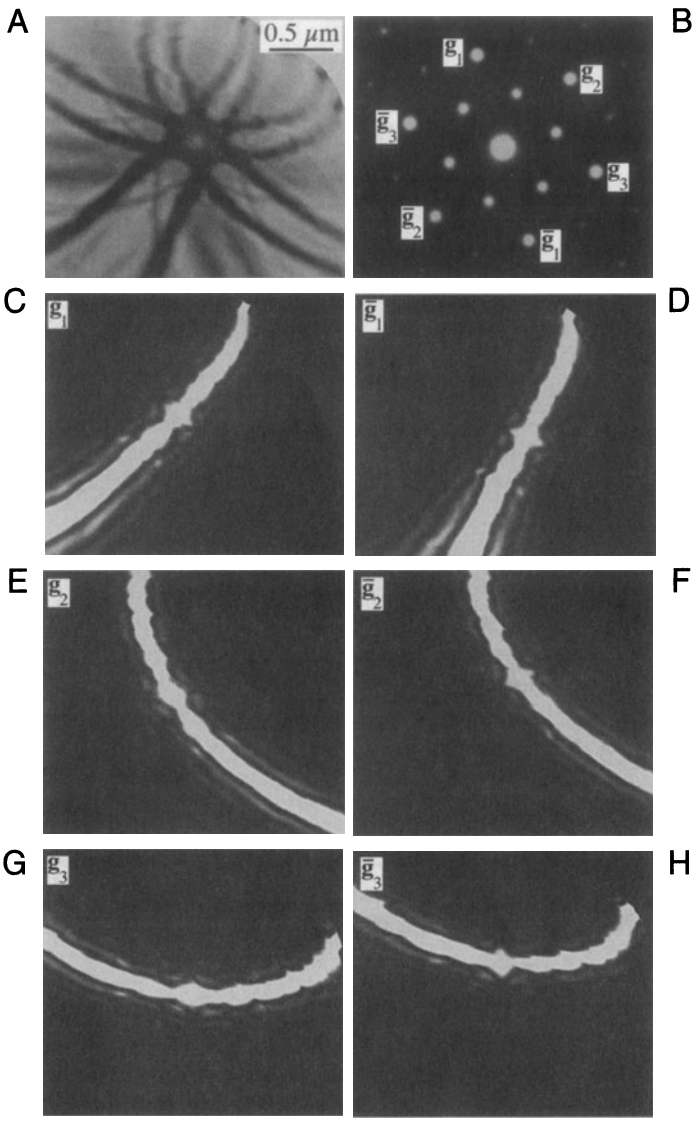

Figure 23.9. An 0001 real space ZAP of Al_2O_3: (A) BF image and (B) corresponding DP. (C–H) Displaced-aperture DF images taken from the spots indicated in (B) identifying the principal dark bend contours in (A); (C,D) $\pm(\bar{3}030)$, (E,F), $\pm(\bar{3}300)$, (G,H) $\pm(03\bar{3}0)$. Note in (A) that the inner $\{11\bar{2}0\}$ spots produce fainter bend contours than the $\{\bar{3}300\}$.

23.7. ABSORPTION EFFECTS

When your specimen is very thick you won't see an image, so we can say that the electrons have then all been absorbed. The absorption process is more important than this obvious statement might imply. Much of our thinking about this topic is, however, just as empirical. In fact, it is common to define an imaginary component ξ_g' to the extinction distance, so

$$\xi_g^{abs} = \xi_g \left(\frac{\xi_g'}{\xi_g' + i\xi_g} \right) \qquad [23.3]$$

in the Howie–Whelan equations. The term ξ_g' is found to be approximately $10\xi_g$. The reason for choosing this expression for ξ_g^{abs} is that the $1/\xi_g$ in the Howie–Whelan equation is replaced by $(i/\xi_g' + 1/\xi_g)$. We do the same for ξ_0. The result is that γ in the Howie–Whelan equations has an imaginary component. Consequently, we now have an exponential decay of the diffracted amplitude. It's a completely phenomenological treatment, but you will see reference to it. When we discuss EELS in Part IV, you'll appreciate the difficulties in modeling the effects of inelastic scattering on the image by a single parameter.

We did briefly discuss absorption of Bloch waves in Chapter 14. We showed that Bloch wave 2 (smaller **k**) is less strongly absorbed than Bloch wave 1; Bloch wave 1 travels along the atom nuclei while Bloch wave 2 channels between them. As the crystal becomes thicker we lose

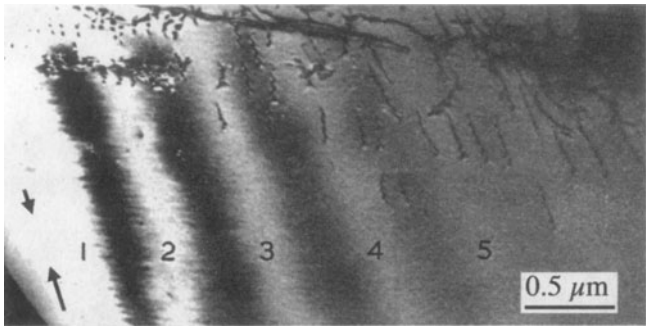

Figure. 23.10. The contrast of thickness fringes in a two-beam BF image decreases when the effect of anomalous absorption is included. Note that the defects are still visible when the fringes have disappeared at a thickness of ~5 ξ_g.

Bloch wave 1. Since thickness fringes result from a beating between the two waves, we will lose the thickness fringes but will still be able to "see through" the specimen, as you can appreciate from Figure 23.10.

Absorption due to the loss of Bloch wave 1 is called anomalous absorption for historical reasons, not because it is unexpected.

Bend contours in thicker parts of the specimen will also show the effect of this anomalous absorption. Looking back at Chapter 15 on the dispersion surface, you'll see that when $\mathbf{s}_g$ is negative the tie line D_1D_2 would be closer to **0** than **g,** and Bloch wave 2 contributes to ϕ_g more strongly. When $\mathbf{s}_g$ becomes positive, Bloch wave 1 is the more strongly excited. We lose Bloch wave 1 because the specimen is thick. So as we rock through the Bragg condition on the bend contour, we'll lose the thickness fringes faster where Bloch wave 1 was weaker already, i.e., when $\mathbf{s}_g$ is negative or inside the ±**g** pair of bend contours.

We can summarize this brief description of absorption with some conclusions:

- We can define a parameter ξ_g' which is usually about $10\xi_g$ and is really a fudge factor that modifies the Howie–Whelan equations to fit the experimental observations.
- The different Bloch waves are scattered differently. If they don't contribute to the image, we say that they were absorbed. We thus have anomalous absorption which is quite normal!
- Usable thicknesses are limited to about $5\xi_g$, but you can optimize this if you channel the less-absorbed Bloch wave.

23.8. COMPUTER SIMULATION OF THICKNESS FRINGES

The simulation of thickness fringes can be carried out using the Head *et al.* programs or with Comis (see Section 1.5). We'll talk more about these programs in Chapter 25, but be wary: don't use a program as a "black box." Why do we need to simulate thickness fringes? As an illustration, let's look at a 90°-wedge specimen (see Section 10.6) so that we know how the thickness changes with position. The actual thickness will be *very* sensitive to the orientation of the specimen since the specimen is so thick, as shown in Figure 23.11A. The specimen is a GaAs/Al_xGa_{1-x}As layered composite grown on (001). Since the cleavage surface it {110} it can be mounted at 45° so the beam is nearly parallel to the [100] pole. The value of ξ_g is different for the two materials, so they can be readily distinguished. Clearly, a quantitative simulation of this situation is nontrivial, especially if you also have to consider the effect shown in Figure 23.6.

Because the fringe spacing changes as ξ_g changes, it will also change if you vary the accelerating voltage. You can see this effect clearly in Figures 23.11B and C which compare the same region of a wedge specimen imaged at 300 kV and 100 kV.

23.9. THICKNESS-FRINGE/ BEND-CONTOUR INTERACTIONS

It's clear from equation 23.1 that both bending and thickness effects can occur together. This combined effect is shown in Figure 23.12, where the axis of bending runs normal to the edge of the wedge specimen. When $\mathbf{s} = 0$, the value of ξ_{eff} is largest. As we bend away from the Bragg condition, on either side, ξ_{eff} decreases so the thickness contours curve toward the edge of the specimen. This image actually shows the **g**(111) and ($\bar{\mathbf{g}}$)($\bar{1}\bar{1}\bar{1}$) contours (arrowed). As an exercise you can calculate the value of **s** at any point between the contours in this image. Assume the wedge angle is constant and $t = 0$ at the edge; then compare the thickness you deduce using ξ_{eff} with the thickness value extrapolated from the regions where $\mathbf{s} = 0$.

If a defect causes the specimen to bend, then the contrast from the defect and that from thickness variations will be linked.

Since the effective thickness is s_{eff}^{-1}, it will change as you increase the deviation parameter, **s**. You can use this fact to determine the thickness of an area quite accurately, providing you have a reference value such as zero thick-

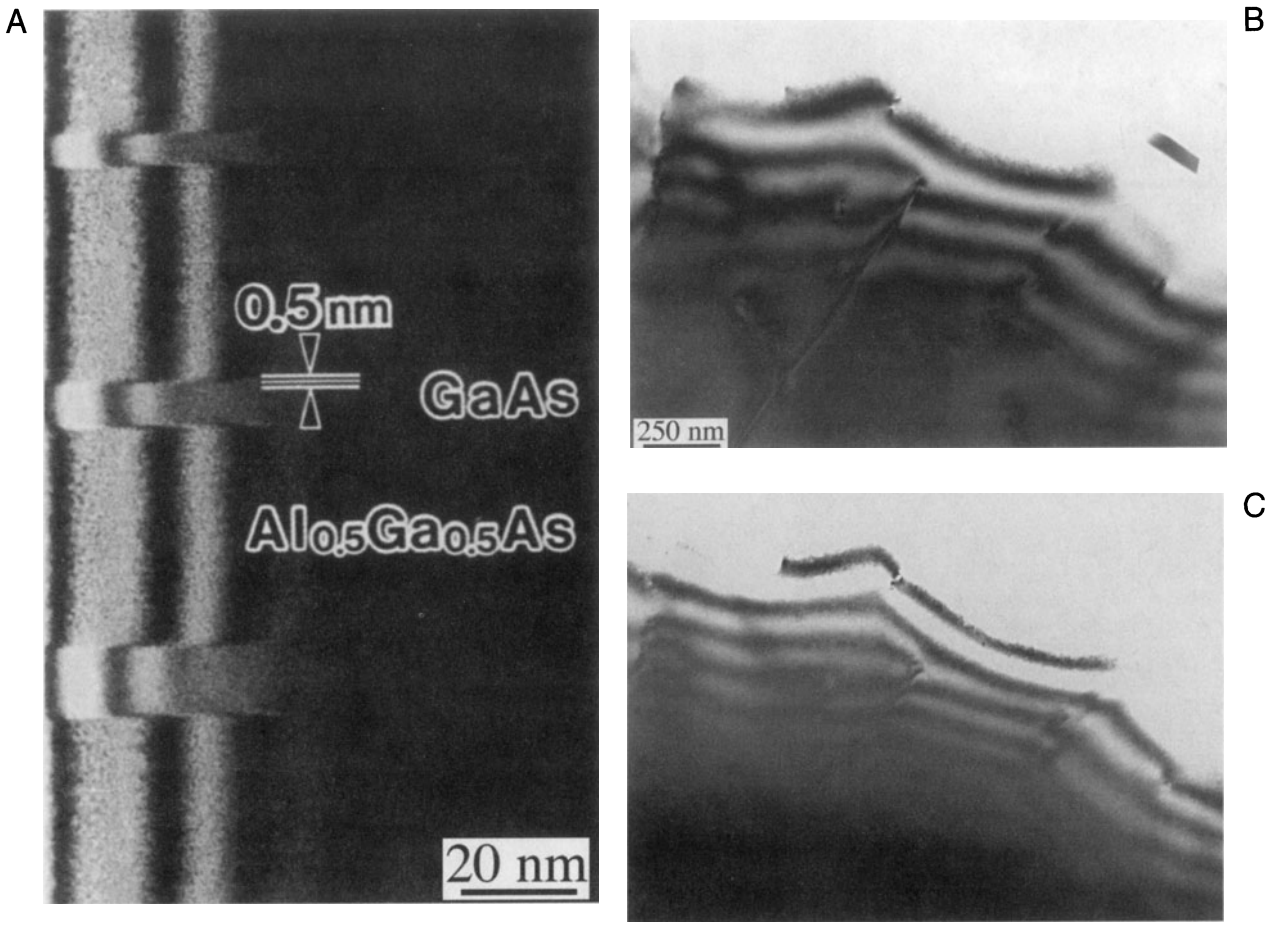

Figure 23.11. (A) Thickness fringes in a 90° wedge of alternating GaAs and AlGaAs. The extinction distance changes in each phase so the fringe spacing changes. Strong beam BF images ($\mathbf{s} = 0$) for (B) 300-kV and (C) 100-kV electrons. The extinction distance increases as the accelerating voltage increases, and you can see through thicker areas; compare with the images in Figure 23.1.

ness at a hole in the specimen. You initially tilt the specimen so that the chosen reflection is at the Bragg condition. (Remember that this analysis assumes that you only have two beams.) You can determine $\mathbf{s}_g$ quite accurately if you can see the Kikuchi lines. Then you can determine s_{eff}^{-1} at different positions on the specimen. The maximum value of s_{eff}^{-1} is ξ_g and occurs at $\mathbf{s}_g = 0$. As you tilt the specimen to increase $\mathbf{s}_g$ in the positive or negative sense, you'll see the thickness fringes move closer together. We'll examine the situation where $\mathbf{s}_g$ is very large in Chapter 26, and where the foil also bends in Section 23.11.

Aside: *You should be careful when using this method for thickness determination in XEDS analysis, since only the thickness of the diffracting (crystalline) material is determined. There may be amorphous material on the surface which has similar or different composition.*

23.10. OTHER EFFECTS OF BENDING

In some situations, the bending of the foil may be more subtle. For example, strains in TEM specimens may relax at the surface of the thin specimen. A particularly important example of this effect was found by Gibson *et al.* (1985) in the study of superlattices in semiconductors.

We'll generalize the situation a little. Imagine that two cubic materials, which normally have slightly different lattice parameters, are grown on one another to form an artificial superlattice with a (001) (i.e., cube-on-cube) interface plane. One crystal must expand and the other contract normal to this interface. When we prepare a cross-section TEM specimen, we might then imagine it relaxing at the surface as shown in Figure 23.13B. The reason for the relaxation is simply that this allows the one material to expand while the other contracts; the constraint at the surface has been removed during the specimen preparation pro-

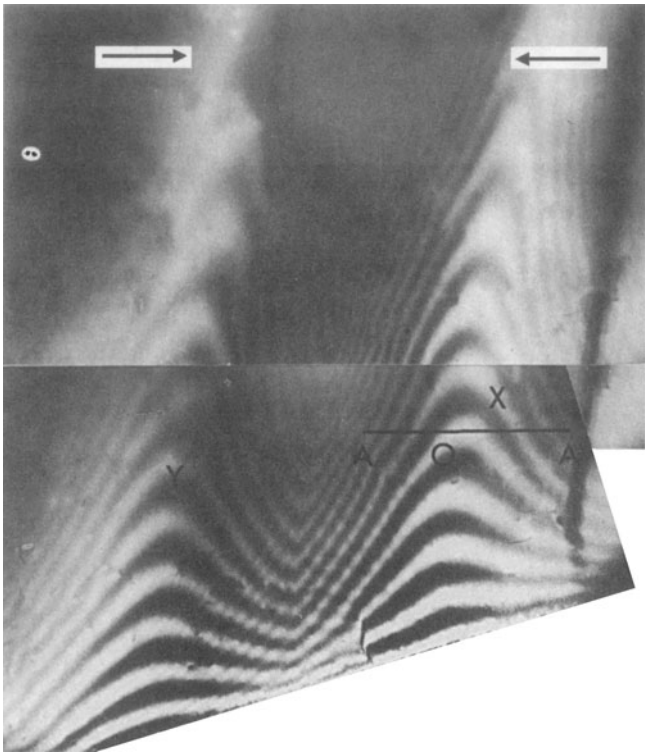

Figure 23.12. Since both thickness fringes and bend contours (X and Y) affect the contrast seen in the image, and both can occur in the same part of the specimen, they can affect, or couple with, one another to give the complex contrast shown in this BF image. Along the line A-A, s changes in sign, being approximately zero at O and negative between the contours.

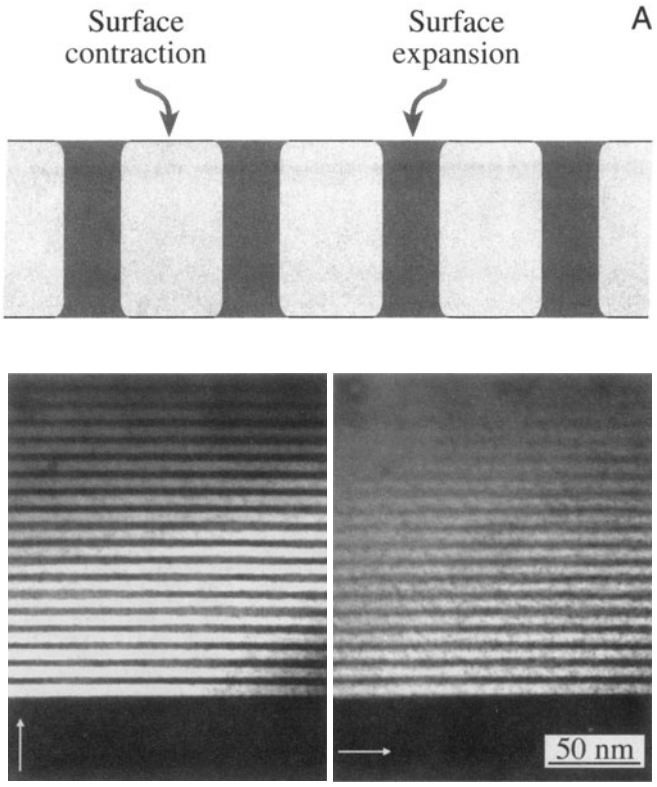

Figure 23.13. (A) A schematic of how interfaces might relax at the surface of a thin specimen. (B,C) DF images of a GaAs/AlGaAs superlattice imaged in two orthogonal reflections, 200 and 020, with the specimen oriented at the 001 pole. (B) The [020] vector is parallel to the interface while (C) the [200] is normal to it. If planes parallel to the interface bend to relax the strain caused by the lattice misfit, then only the 020 image will be affected, giving a more abrupt contrast change.

cess. This argument is admittedly crude, but Figures 23.13B and C show that images recorded with $\mathbf{g} = 020$ normal to this interface appear sharper than images formed when $\mathbf{g} = 200$ is parallel to the interface.

So, no matter whether $\mathbf{g}$ is 020 or $0\bar{2}0$, the Bragg planes are bent closer to $\mathbf{s} = 0$ at one surface or the other.

Here, bending only occurs within a short distance of the interface but it significantly affects the appearance of the DF image. The bending is actually making the image appear sharper than it should.

This example is special but emphasizes the point: relaxation at the surface can cause the specimen to bend and this bending will affect the appearance of your image.

CHAPTER SUMMARY

The effects of changes in thickness and specimen bending are both explained by equation 23.1. Although this equation was derived for a two-beam geometry, you'll see similar effects when more strongly excited beams are present but the simple $\sin^2$ dependence will be lost.

- Varying t while keeping $\mathbf{s}$ constant gives thickness fringes.
- Varying $\mathbf{s}$ while keeping t constant gives bend contours.

Thickness fringes are an interference effect and, with care, can be used to calculate the foil thickness and reveal the topography.

Note that if the two surfaces of the specimen are parallel, then we don't see thickness fringes, even if the specimen is tilted. However, the contrast of that region will depend on the projected thickness.

Bend contours are very useful because they map out the value of **s** in the specimen. If your foil is bent around more than one axis, bend contours combine to produce beautiful ZAPs which reflect the true symmetry of the material.

However, if you want to keep defect analysis simple, then you need to avoid bending and work in relatively thin regions of nearly constant thickness. The exception to this rule is that there are quite a few special cases where you want to do exactly the opposite! So the message is that bending and thickness variations give you extra parameters which you can use in your study as long as you can control these parameters. This control comes from mastering the BF/DF/SAD techniques in Chapter 9.

Lastly, be aware that anomalous absorption is not anomalous. It can best be explained by Bloch-wave interactions.

REFERENCES

Specific References

Gibson, J.M., Hull, R., Bean, J.C., and Treacy, M.M.J. (1985) *Appl. Phys. Lett.* **46**, 649.

Rackham, G.M. and Eades, J.A. (1977) *Optik* **47**, 227.

Susnitzky, D.W. and Carter, C.B. (1992) *J. Am. Ceram. Soc.* **75**, 2463. An overview of the surface morphology of heat-treated ceramic thin films studied using TEM.